Classification of visual strategies in human postural control by stochastic parameters

Lorenzo Chiari *, Andrea Bertani, Angelo Cappello

Biomedical Engineering Unit, Department of Electronics, Computer Science and Systems, University of Bologna, Viale Risorgimento, 2, 40136 Bologna, Italy

Abstract

In a significant proportion of individuals, the expected increase of body sway upon eye closure is not actually observed. This result prefigures different visual contributions to the fine regulation of body sway. The present paper documents a method to classify healthy subjects into one visual or non-visual group according to the fractal properties of center of pressure (COP) profiles. The recognition of the sensory strategy consists of several phases: first, stabilogram diffusion analysis is carried out on the time-series of COP; then, stochastic features are extracted by two models of different complexity. In particular, a new technique is proposed which describes with continuity the transition among different scaling regimes. Finally, a linear classifier is designed. The method gave very high performance classifying, with the best set of features, provided by the two parameters of the new model, 93.3% of the examined subjects in agreement with the preclassification, provided by percentage difference of sway between eyes open and eyes closed conditions and computed over the area of the 95% confidence ellipse. © 2000 Elsevier Science B.V. All rights reserved.

PsycINFO classification: 2320; 2330; 2240

Keywords: Postural control; Vision; Human postural sway; Stochastic processes; Statistics

---

* Corresponding author. Tel.: +39-051-209-3014; fax: +39-051-209-3073.
  E-mail address: lchiairi@deis.unibo.it (L. Chiari).

1. Introduction

The control of human posture is a multisensory process in which the central nervous system integrates several pieces of afferent information. The aim of the nervous system is the estimation of body segments' orientation relative to each other and to the a priori unknown surrounding environment. Consequently it properly drives the musculo-skeletal structure in order to maintain or achieve the desired orientation in space, and hence postural stability.

In detail, the vestibular system provides information regarding accelerations of the head in space (Horak, Shupert, Dietz, & Horstmann, 1994). The somatosensory system provides proprioceptive information that can be used to determine changes in body position (Inglis, Horak, Shupert, & Jones-Rycewicz, 1994). Furthermore, graviceptors exist in the trunk that can be used to detect changes in the orientation of the subject with respect to gravity (Mittelstaedt, 1996). However, of all different sources of information available, the visual system is of central importance. It senses position and velocity of the head and has a crucial role in stabilizing posture (Dichgans, Mauritz, Allum, & Brandt, 1976), providing the most sensitive mean of perceiving sway during normal standing (Lacour et al., 1997). The functional contribution of all these afferent control loops to detection of position and motion has been reviewed by Fitzpatrick and McCloskey (1994).

An important aspect, which is still under debate in the literature, concerns sensory integration: it is well accepted that in normal subjects, feedback information from different subsystems is redundant but complementary, and contributes in several ways to body sway stabilization. Nevertheless, the interconnection of the multiple feedback paths involved in postural control is not yet completely understood. However, the particular integration pattern that a subject puts into play during quiet standing can be definitely viewed as a sensory strategy. Hence, as a result of redundancy and plasticity, several strategies may be found in subjects that can rely on all sensory loops. In particular, two main classes of subjects were identified in literature on the basis of differential contribution of static visual cues to the fine regulation of posture.

A majority of subjects shows an increased sway when tested under eyes-closed conditions. On the contrary, a second class of subjects, sometimes referred to as *postural blind* (Marucchi & Gagey, 1987), sways less when eyes are closed than when eyes are open. Several authors reported such finding, both in health (Lacour et al., 1997; Van Parys & Njiokiktjien, 1976; Black,

Wall, Rockette, & Kitch, 1982) and disease (Black, 1982; Gagey & Toupet, 1991; Lacour et al., 1997). They quantified postural sway by summary statistic scores extracted from center of pressure (COP) time-series, that is the location of the resultant of the ground reaction forces produced during standing. COP is commonly measured by means of a force platform, and is supposed to reflect some internally generated perturbations and the action of the overall postural control system (Myklebust, Prieto, & Myklebust, 1995). A thorough review of such scores can be found in Prieto, Myklebust, Hoffmann, Lovett, and Myklebust (1996); unfortunately some limitations occur since these parameters are univariate descriptors of body sway and do not aspire to assess the dynamic properties of the COP.

Actually, COP displacements during human standing display a fractal behavior (Duarte & Zatsiorsky, 2000). This important property, common to many physiological processes, can be expressed in terms of *statistical self-similarity*. Such self-similarity implies that there is a *scaling relationship* describing how the measured value of a statistical property depends on the scale at which it is measured. The simplest scaling relationship determined by self-similarity has a power law form, leading to a straight line on log–log plots. An exhaustive tutorial and a wide review of fractal phenomena in physiology can be found in the book by Bassingthwaighte, Liebovitch, and West (1994).

In the analysis of COP experimental data the existence of scaling comes to light, for example, if the variance of the displacements (i.e., the distances between consecutive points of the planar COP time-series) is examined over different timescales. One main implication of fractality is that scaling functions that describe how the values change with the resolution tells more about the data than the value of the measurement at any one resolution (in particular, at the higher resolution as it is commonly done by the summary statistic scores, working with the original sampled time-series). For this reason, to obtain more significant parameters about the postural control system, techniques postulating the timescale dependence of COP statistical properties have been recently proposed in the literature. Collins and De Luca (1993) were the first who characterized the fractal properties of COP time-series during quiet stance using a framework of classical and fractional Brownian motion (Mandelbrot & Van Ness, 1968). In this way, they showed that COP fluctuations have a structure that is dependent upon the timescale of observation and not simply random. In particular, they found that the scaling laws needed to accurately model the phenomenon in the range 0.01–10 seconds were at least two. They interpreted the results by proposing two

modes of postural control taking place over different periods of time: open-loop and feedback.

The work by Collins and De Luca was promising in terms of postural sway characterization and seminal for following studies. Nevertheless, it is accepted opinion that this method could be further developed to better address some technical drawbacks about parameter estimation, and to investigate its impact on postural control theories (Newell, Slobounov, Slobounova, & Molenaar, 1997).

In a previous paper, we proposed an improvement in the parameter estimation technique, reducing from six to four the number of parameters needed to characterize the data set. We assumed a unified theory in which a two-region multi-scale fractional Brownian motion was identified, and classical Brownian motion was not required (Chiari, Cappello, Lenzi, & Della Croce, 2000). Parameter reliability and sensitivity to visual input were consequently improved. In this paper we develop a new technique, aimed at describing with continuity the transitions among the different scaling regimes found in COP time-series. This means that the tool that is proposed will not make a priori assumptions on the number of scaling laws to be identified on COP data. In this way, any possible transition becomes part of the model, and the multi-scale fractional Brownian motion (Benassi & Deguy, 1999) has infinite possible regimes, as can be seen, for example, when estimating the local scaling properties over small ranges of time intervals (Liebovitch & Yang, 1997). This approach has the significant advantage of further reducing the number of parameters.

While stochastic features have already found a significant role in data analysis (Riley, Wong, Mitra, & Turvey, 1997; Newell et al., 1997) and starting to be used for physical modeling (Chow, Lauk, & Collins, 1999), the present study aimed at assessing the capability of the novel parameters in the pattern recognition of the different visual strategies used by a population of healthy adults. In this light, what is important for a model is its ability to properly classify subjects coherently with clinical experience. The idea is that, hopefully, the more a single model is a good descriptor of different observations (strategies), the more its parameters could be seen as meaningful markers of the underlying physiological control process, at least for the aspects which are involved in that particular concern.

The way in which visual input affects the postural performance is investigated through a classification approach that employs: (i) *fuzzy clustering*, as a surrogate of a priori knowledge, for the preclassification of visual strategies; (ii) *stochastic process modeling* of COP trajectories as a valid feature

extraction scheme; (iii) *discriminant analysis* through a parametric Bayes classifier, for testing the sensitivity and comparing the performances of new stochastic parameters to different patterns observed during the Romberg test.

2. Materials and methods

2.1. Experimental methods

Experiments were carried out on 60 healthy adults (43 females and 17 males; mean age ± std: 37 ± 10 years; range: 21–64 years) while standing upright on a force platform with arms at the side. Subjects were instructed to look at a small achromatic target (circular, with a diameter of 3 centimeters), placed at eye height, about 3 meters from the platform, and to stand in a comfortable stance. Romberg test was performed, i.e. trials were carried out with both eyes open (*eo*) and eyes closed (*ec*). None of the subjects had evidence or known history of neuro-musculo-skeletal disorder. Informed consent was obtained prior to the inclusion in the study.

Each experimental session was composed of four tests, two performed with the eyes open and two with the eyes closed. The posturographic recordings, each consisting of a 50-second acquisition, alternated *eo* and *ec* conditions. COP coordinates were measured by a multi-component strain gage force platform (mod. 4060-08, Bertec Corporation) and sampled at a frequency of 20 Hz. Fig. 1 shows representative 50-second recordings obtained with eyes open and eyes closed for both classes of subjects. The antero-posterior component of sway (y_{COP}) is plotted against the corresponding medio-lateral component (x_{COP}).

All the steps of the classification procedure, including data acquisition, were managed and designed on a Pentium II PC mounting Matlab 5.3 and its Data Acquisition Toolbox (The Mathworks). Hypothesis testing was performed by means of NCSS 2000, and the most appropriate statistical tests were used, according to the properties of the variables under study.

2.2. Fuzzy clustering preclassification

The most common index used to quantify the influence of visual input on postural performance is the Romberg Quotient (RQ):
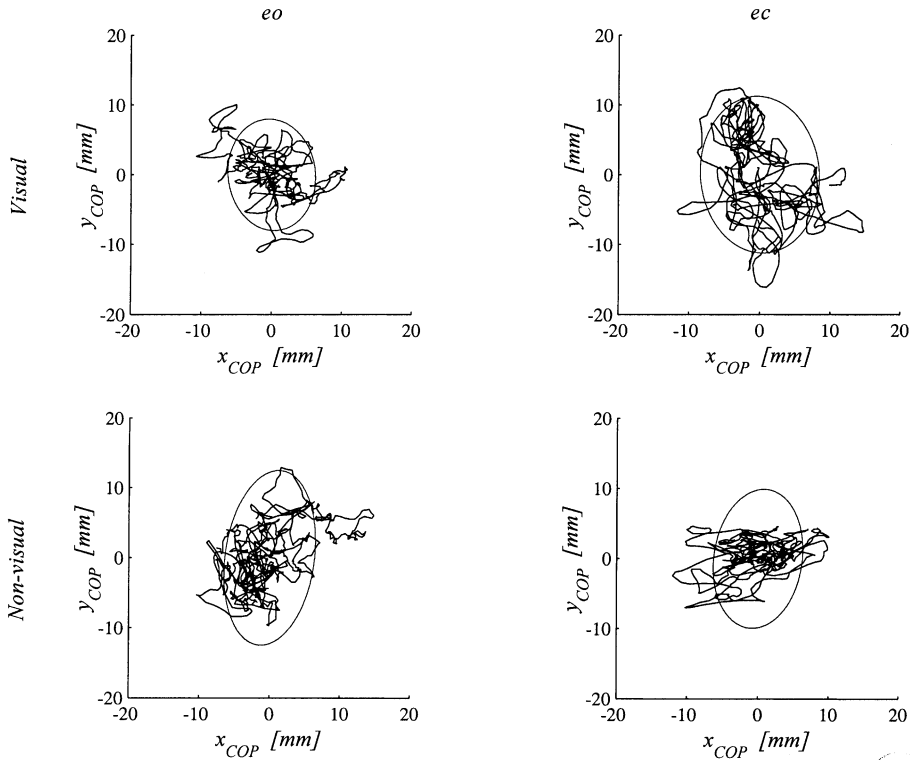
Fig. 1. Typical time courses of the two components of COP: mediolateral (x_{COP}) and anteroposterior (y_{COP}). Four trials are shown: two with eyes open (*eo*) – left panels, and two with eyes closed (*ec*) – right panels. Upper panels refer to a Visual subject while lower panels refer to a Non-visual subject. Estimated 95% CEA's are also shown.

$$RQ = \frac{\text{score}(ec)}{\text{score}(eo)}, \tag{1}$$

where the score can be any valid measure of postural sway (Van Parys & Njiokiktjien, 1976).

Recently, a new index was proposed which is a nonlinear function of the former, but is preferable for putting in light the possible presence of bimodal distributions in data (Lacour et al., 1997). It is the percentage difference of sway (PDS) and is nothing but the ratio

$$PDS = \frac{RQ - 1}{RQ + 1} 100. \tag{2}$$

A ratio close to zero or negative indicates that the magnitude of body sway is similar or smaller in the *ec* than in the *eo* condition. On the contrary, positive values reflect a larger sway in the *ec* than in the *eo* condition.

The summary statistic score we used to measure postural sway was the 95% confidence ellipse area (CEA), that is the area of the 95% bivariate confidence ellipse that is expected to enclose approximately 95% of the points on the COP path (Prieto et al., 1996).

To test the evidence that healthy subjects follow a visual (V) or non-visual (NV) strategy, we submitted the mean PDS data to a 1-D cluster analysis. This procedure was used as independent statistical criterion and was performed by the fuzzy clustering algorithm described in the following (Bezdek, 1981).

Fuzzy techniques are very popular in biomedical research since hard labeling is often not successful in finding clusters in real world data, where class membership is not crisp. It is common experience that the boundaries between classes of real objects are in fact badly delineated, and it seems more realistic to assign to each pattern $\mathbf{x}$ a set of membership values, one for each group, rather than a single label (Bezdek, 1998). The most widely used objective function for fuzzy clustering in $\mathbf{X} = \{\mathbf{x_1}, \mathbf{x_2}, \ldots, \mathbf{x_n}\}$ is the weighted within groups sum of squared errors:

$$J(W, \mathbf{P}) = \sum_{j=1}^{n} \sum_{i=1}^{c} (w_{ij})^m d^2(\mathbf{x_j}, \mathbf{p_i}) \tag{3}$$

where w_{ij} is the fuzzy membership of the pattern $\mathbf{x_j}$ to class i, $\mathbf{P} = \{\mathbf{p_1}, \mathbf{p_2}, \ldots, \mathbf{p_c}\}$ is a matrix of (unknown) cluster centers, $m \geqslant 1$ is the degree of *fuzzification* of the clusters (generally $m = 2$; with $m = 1$ the algorithm becomes the well-known "hard" clustering *nearest mean*), and $d^2(\mathbf{x_j}, \mathbf{p_i})$ is a squared distance between $\mathbf{x_j}$ and $\mathbf{p_i}$.

By defining the Euclidean metric $d^2(\mathbf{x_j}, \mathbf{p_i}) = (\mathbf{x_j} - \mathbf{p_i})^{\mathrm{T}}(\mathbf{x_j} - \mathbf{p_i})$, the objective function J can be minimized under the following necessary conditions:

$$w_{ij} = \left(\frac{1}{d^2(\mathbf{x_j}, \mathbf{p_i})}\right)^{1/(m-1)} \bigg/ \sum_{k=1}^{c} \left(\frac{1}{d^2(\mathbf{x_j}, \mathbf{p_k})}\right)^{1/(m-1)} \tag{4}$$

and

$$\mathbf{p_i} = \frac{\sum_{j=1}^{n} (w_{ij})^m \mathbf{x_j}}{\sum_{j=1}^{n} (w_{ij})^m}. \tag{5}$$

The approximate optimization of J is then obtained recursively:

1. for each pattern $\mathbf{x_j} \in \mathbf{X}$ randomly initialize memberships, w_{ij}, such that

$$0 \leqslant w_{ij} \leqslant 1, \quad 1 \leqslant i \leqslant c \text{ and } \sum_{i=1}^{c} w_{ij} = 1; \text{ pose } \hat{w}_{ij} = w_{ij};$$

2. calculate the cluster centers with Eq. (5);
3. compute the new membership values with Eq. (4);
4. if $\max_{ij} |w_{ij} - \hat{w}_{ij}| < \varepsilon$ then stop, otherwise pose $\hat{w}_{ij} = w_{ij}$ and iterate through 2.

The algorithm always converges to a local minimum, generally within a few iterations Bezdek (1981, p. 80), even if different choices of initial w_{ij} might lead to different local minima. For this reason it is a common practice to run the optimization algorithm several times in order to find the best local minimum of J. Since a definite class assignment is the ultimate goal of clustering, the outputs of the fuzzy algorithm are finally transformed into crisp labels. This is called *defuzzification* and is obtained by the maximum membership rule (i.e., each pattern is assigned to the cluster with the maximum membership) (Bezdek, 1998).

One of the most difficult tasks in cluster analysis is to choose the appropriate number of clusters. Kaufman and Rousseeuw (1990) defined a set of values called *silhouette coefficients*, SC, ranging from −1 to 1, which measure how well each single pattern has been classified by comparing its dissimilarity within its cluster to its dissimilarity with its nearest neighbor. In particular, they proposed to interpret values of SC higher than 0.70 and in the range 0.51–0.70 as markers of a strong and a reasonable structure captured in the data, respectively.

In fuzzy clustering there are a number of indirect validity indices that can be used in conjunction with the crisp silhouette values as measures of partition (W) quality. A geometric rationale (good clusters should have compact representations and wide separations) induced Xie and Beni (1991) to define an index of fuzzy cluster validity such that the smaller it is, the more separate are the clusters:

$$XB(W, \mathbf{P}) = \frac{1}{n} \frac{\sum_{j=1}^{n} \sum_{i=1}^{c} w_{ij}^2 d^2(\mathbf{x_j}, \mathbf{p_i})}{\min_{i \neq k} \{d^2(\mathbf{p_k}, \mathbf{p_i})\}}. \tag{6}$$

Good clusters should maximize SC and minimize XB.

2.3. Stochastic feature extraction

Several simple random walk models can produce fractal time-series with properties similar to the ones of postural sway. The implicit underlying assumption is that the movement of the COP represents the combined output of coexistent deterministic and stochastic mechanisms.

The consequent fractal analysis gives the instruments for feature extraction. First we calculate the variance of the 2-D displacements, Δr, and determine how the variance diverges with time. For COP time-series this method is commonly called *stabilogram diffusion analysis* (Collins & De Luca, 1993).

By definition, in presence of a fractional Brownian motion (Mandelbrot & Van Ness, 1968), the relation between variance and time interval, $V(\Delta t)$, should follow a simple exponential scaling law:

$$V(\Delta t) = \langle \Delta r^2 \rangle - \langle \Delta r \rangle^2 \sim \Delta t^{2H}, \tag{7}$$

where brackets indicate a time average, Δt is the time increment and H is the scaling exponent. This is also called Hurst exponent (Hurst, 1951) and represents the rate of correlation decay that characterizes the random process; it can be any real number between 0 and 1 and the lower it is the more jittery the process is. In particular, such coefficient provides the following information about correlation:

- when $H = 0.5$ the values of the time-series are uncorrelated with each other;
- when $0 < H < 0.5$ the values of the time-series are said to be "antipersistent" because increases are more likely to be followed by decreases;
- when $0.5 < H < 1$ the values of the time-series are said to be "persistent" because increases are more likely to be followed by increases.

The relation between $V(\Delta t)$ and Δt is known as the stabilogram diffusion function (SDF) and can be depicted both in linear and bi-logarithmic scales. A representative log–log SDF can be seen in Fig. 2. The term $\langle \Delta r \rangle^2$ in Eq. (7) is often negligible so that in place of $V(\Delta t)$ one can also consider the scaling law on $\langle \Delta r^2 \rangle$ (mean square displacements) with no loss in generality.

Previous studies suggested that even simple models are able to describe the greatest part of the variance of the SDF (Chiari et al., 2000; Newell et al., 1997) and, as a corollary, this increases the reliability of the respective parameters. For this reason, in order to compare the information carried by the features of models of different complexity, we decided to describe the log–log SDF also through a new curve, which is still on the furrow of the fractal
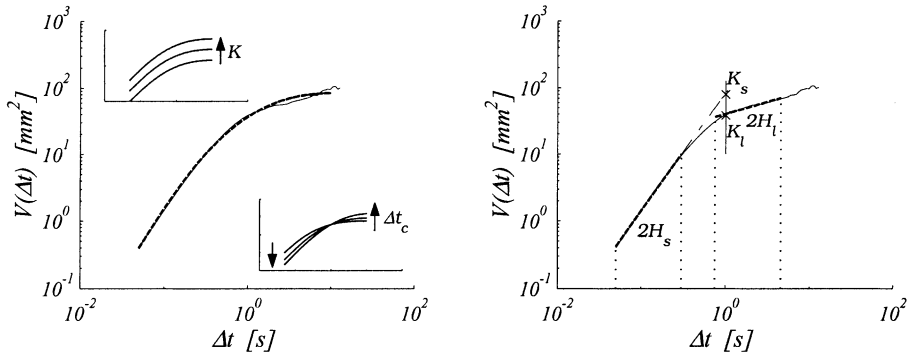
Fig. 2. Representative log–log SDF (solid line). The fitting strategies (dotted lines) and the geometrical meaning of different stochastic parameters are shown. The arrows denote the effect of an increase of the specified parameter. Left panel: sigmoid (Σ) model. Right panel: piecewise linear (PWL) model.

approach by Collins and De Luca, but reflects the continuous changes in correlation. The framework is formally similar to the fractional Brownian motion, but exponent H follows a sigmoid law in time interval Δt:

$$V(\Delta t) = K\Delta t^{2H(\Delta t)} \tag{8}$$

with

$$H(\Delta t) = \frac{\log 2}{\log [2(1 + \Delta t/\Delta t_c)]}. \tag{9}$$

This choice was dictated by the observation that a unique Hurst coefficient could not be defined for the entire process and a significant transition between different scaling regimes takes place in data taken from postural sway. A similar pattern can be seen in Liebovitch and Yang (1997), Fig. 2(d). In particular, for small time intervals, H (i.e., half the slope of SDF in log–log scale) approaches 1, while for time intervals commonly greater than 1 second, H drastically decreases and it approaches 0 as $\Delta t \to \infty$. Since this transition from persistent to antipersistent correlation takes place with continuity, a sigmoid shape was retained a suitable description of the different regimes. On this basis in the following we will refer to this model with the name Σ.

In this way the features extracted from COP data are only two: K and Δt_c. Parameter K is the variance of the displacements for $\Delta t = 1$ second, which is also proportional to the variance of the displacements for large time-lags ($V(\Delta t) \to 4K$ as $\Delta t \to \infty$). Since $V(\Delta t_c) = K\Delta t_c$, K can be thought of as an

estimate of the actual diffusion coefficient of the random process which is encountered by sampling the time series Δr at a sampling frequency $1/\Delta t_c$. In fact, parameter Δt_c is the midpoint of the sigmoid and represents the time-lag in which $H = 0.5$, corresponding to a purely random behavior. In this sense it is an estimate of the time-lag at which the real process switches from a persistent (positively correlated) to an antipersistent (negatively correlated) behavior. The approximation of a representative SDF with model Σ and the relative influence of its parameters on the curve are shown in Fig. 2.

Fig. 2 also depicts the parameterization descending from Collins and De Luca piecewise linear (PWL) approach that is here considered for comparison (Chiari et al., 2000). In this model the nonlinearity of the SDF (i.e., the presence of more than one scaling law) was dealt with by isolating the short- and long-term regions. The geometrical meaning of corresponding parameters is sketched in the right axes of Fig. 2. In fact, $2H_s, 2H_l$ are the slopes of the two best-fitting lines, and K_s, K_l are the intercepts for $\Delta t = 1$:

$$\log V(\Delta t) = \begin{cases} 2H_s \log \Delta t + K_s & \text{for } \Delta t \leqslant \tau, \\ 2H_l \log \Delta t + K_l & \text{for } \Delta t > \tau, \end{cases} \tag{10}$$

where τ is a dependent parameter (Chiari et al., 2000):

$$\tau = \left(\frac{-K_l}{K_s} \right)^{\frac{1}{2(H_s - H_l)}}. \tag{11}$$

For both models, a least-squares algorithm was used for parameter estimation from log–log SDF.

2.4. Discriminant analysis

The effectiveness of the preclassification assumption (i.e, two visual strategies exist on the basis of PDS computed on 95% CEA) was tested on the space of the stochastic parameters and the results of the different models were compared.

A linear classifier with optimum design (LCOD) assessed class separability in the space of the features and its performance was evaluated by the *leave-one-out* (LOO) empirical error counting technique (Fukunaga, 1990).

The choice of a linear classifier is due to its simplicity and robustness and leads to a decision rule like

$$h(\mathbf{x_j}) = \mathbf{v}^T \mathbf{x_j} + v_0 \underset{\omega_2}{\overset{\omega_1}{\underset{<}{\overset{>}{}}}} 0, \quad j = 1, \ldots, n, \tag{12}$$

indicating that pattern $\mathbf{x_j}$ (in this case the vector storing stochastic features) is projected onto vector $\mathbf{v}$ and the resulting variable $(\mathbf{v}^T \mathbf{x_j})$ is classified to either ω_1 or ω_2 depending on whether it is greater or lower than $-v_0$. The optimum design procedure consists in selecting parameters $\mathbf{v}$ and v_0 which give the smallest classification error in the projected space. The classification error is estimated through resubstitution and LOO methods.

The classifier parameters $(\mathbf{v}, v_0)$ are obtained using an iterative procedure made up of the following steps (adapted from Fukunaga, 1990):
1. Compute the sample mean, $\mathbf{M_i}$, and sample covariance matrix, $\mathbf{C_i}$, for the two populations $(i = 1, 2)$.
2. Calculate $\mathbf{v}$ for a given weight s by $\mathbf{v} = [s\mathbf{C_1} + (1 - s)\mathbf{C_2}]^{-1}(\mathbf{M_2} - \mathbf{M_1})$.
3. Compute $y_j = \mathbf{v}^T \mathbf{x_j}$ using the $\mathbf{v}$ obtained at step 2.
4. Compute the resubstitution error and find the v_0 which gives the smallest error.
5. Scan s from 0 to 1 and select the value that gives a minimum LOO error.
In the case of $s = 1/2$ and $v_0 = 0$ the LCOD coincides with the Bayes Linear Classifier.

3. Results

In the present section we review the main issues addressed by our approach in the pattern recognition problem of identifying different visual strategies employed during the Romberg test. The different steps of the classification process are sketched in Fig. 3 and corresponding results are reported in sequence.

3.1. Fuzzy clustering preclassification

In the absence of a priori knowledge provided by an expert about the different kinds of visual integration employed by the subjects under study, a statistical method was used for preclassification of postural patterns. Computation of CEA and corresponding RQ was performed in each couple of
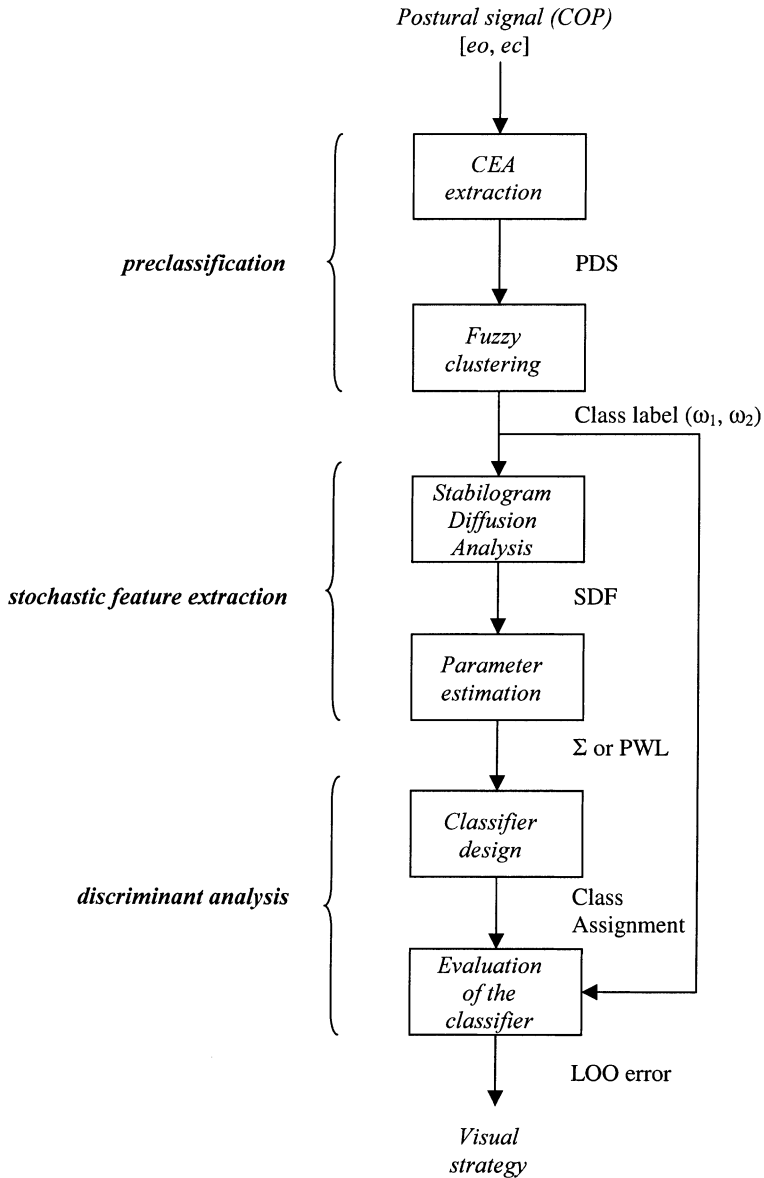
Postural signal (COP)
[*eo, ec*]

Fig. 3. Flow-chart of the pattern recognition system. For acronyms see text.

subsequent eo and ec tests. Hence, a mean PDS was computed for each subject and evidence that the population was not homogeneous was suggested by the resulting distribution. Moreover, both indices used for the

Table 1
Cluster validity indices[a]

	$c = 2$	$c = 3$	$c = 4$
SC	**0.65**	0.50	0.39
XB	**0.12**	0.32	0.65

[a] The values of a crisp (SC) and a fuzzy (XB) index assess the partition quality in the case of $c = 2, \ldots, 4$. The preference for $c = 2$ is well evident.

choice of the number of clusters suggested to look for a bivariate distribution in the 1×60 vector of PDS(CEA). The results of this cluster design phase are shown in Table 1 and demonstrate that the maximum of SC and the minimum of XB are both encountered when $c = 2$. The corresponding value SC $= 0.65$ indicates that a quite strong structure has been captured in the data. Consequently, the fuzzy clustering algorithm splits the population into two well-identified and significantly different clusters. The first group was composed of 19 subjects (31.7%) exhibiting a mean percentage difference of sway of $-12.8 \pm 9.0\%$ S.D. (range -33.1% to -0.1%) that is always below zero. This group, that we will call ω_1, is not significantly helped by vision for postural stabilization and hence can be related to a non-visual strategy. The second group, that we will call ω_2, included the remaining 41 subjects (68.3%), who showed a mean of $15.4 \pm 9.7\%$ S.D. percentage difference of sway (range 3.1%–44.3%). These subjects swayed more in the *ec* conditions and hence used a visual strategy to control their posture. No significant difference in sex and age was found in the composition of the two groups.

Fig. 4 shows the histogram distribution of the PDS and depicts the two groups. A first result of the separation is that the sensitivity of CEA to visual conditions (*eo*, *ec*) measured by a paired *T*-test is largely increased. In fact, the two groups show significant differences between *eo* and *ec* sway ($P < 0.0001$ for both ω_1 and ω_2) that the whole population can get only to a minor extent ($P < 0.01$) due to the partial overlapping of the two strategies.

It is worth noting that the clustering algorithm splits the two groups at around 0% (corresponding to RQ $= 100\%$). In the present population, the same group composition was obtained by clustering the RQ parameter in place of PDS.

3.2. Stochastic feature extraction

The first step of the pattern recognition system design dealt with the problem of extracting a set of features from the available measurements preserving sufficient discriminant information. This was achieved through the
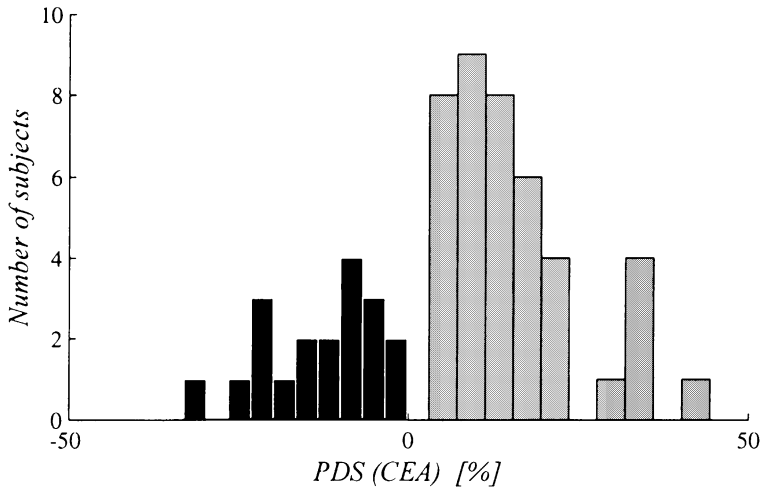
Fig. 4. Fuzzy clustering preclassification results. Visual (gray) and Non-visual (black) groups are clearly separated by a null value of PDS computed over CEA score.

four parameters of PWL and the two parameters of Σ stochastic models of SDF's, even if different models could be eligible (e.g., Newell et al., 1997) and were tested for comparison, as will be discussed in the following. Mean values and standard deviations of the means of the respective features are summarized in Table 2 (PWL model) and Table 3 (Σ model).

As regards PWL, it is a general observation that the short-term parameters are always greater than the corresponding long-term parameters, for both

Table 2
Group means and S.D. for the PWL parameters under eyes open (*eo*) and eyes closed (*ec*) conditions: ω_1 – non-visual, ω_2 – visual group[a]

		eo	*ec*	
ω_1	H_s	0.80 ± 0.03	0.75 ± 0.05	††
	K_s [mm^2]	1.73 ± 0.23	1.77 ± 0.27	
	H_l	0.22 ± 0.07	0.09 ± 0.05	††
	K_l [mm^2]	1.39 ± 0.17	1.52 ± 0.20	†
ω_2	H_s	0.78 ± 0.03	0.77 ± 0.04	
	K_s [mm^2]	1.64 ± 0.24	1.84 ± 0.29	††
	H_l	0.15 ± 0.05	0.12 ± 0.07	†
	K_l [mm^2]	1.34 ± 0.18	1.54 ± 0.22	††

[a] The symbols † and †† denote statistically significant differences between visual conditions at $P < 0.001$ and $P < 0.0001$ levels, respectively.

Table 3
Group means and S.D. for the Σ parameters under eyes open (*eo*) and eyes closed (*ec*) conditions: ω_1 – non-visual, ω_2 – visual group[a]

		eo	*ec*	
ω_1	K [mm^2]	31.81 ± 15.49	33.47 ± 21.74	
	Δt_c [seconds]	0.38 ± 0.24	0.17 ± 0.08	††
ω_2	K [mm^2]	24.29 ± 10.79	35.99 ± 16.18	††
	Δt_c [seconds]	0.25 ± 0.18	0.19 ± 0.10	†

[a] The symbols † and †† denote statistically significant differences between visual conditions at $P < 0.001$ and $P < 0.0001$ levels, respectively.

groups and both visual conditions. This is a direct consequence of the shape of the SDF's, having a steeper ascent in the first part (low time-lags) and a significant flattening before $\Delta t = 1$ second. Moreover, all parameters change in the same direction in both groups due to eyes closure, i.e. H_s and H_l decrease while K_s and K_l increase. Most of these within-groups, between-visual conditions changes have a statistical significance, assessed by a paired T-test and evidenced in Table 1. It is noteworthy that all long-term parameters change significantly and that ω_1 is mainly characterized by the decrease in H_s and H_l with *ec* ($P < 0.0001$) whereas ω_2 is mainly characterized by the increase in K_s and K_l with *ec* ($P < 0.0001$). On the contrary, the only significant difference between-groups, within-visual conditions is due to the higher value of H_l with *eo* in group ω_1 (equal variance two-sample T-test, $P < 0.001$).

At the first glance, the parameters of the Σ model reveal their greater inter-subject variability with respect to PWL model parameters. In fact, standard deviations of the means are about 50% of the respective mean values. K and Δt_c change in the same direction in both groups, due to eyes closure: K increases and Δt_c decreases. The sensitivity to visual conditions within-groups is high and a main difference is remarkable between ω_1 and ω_2 since in turn Δt_c and K is the major responsible, respectively (Wilcoxon rank-sum, $P < 0.0001$). The only difference which is statistically significant between-groups, within-visual conditions (Mann–Whitney two-sample T-test, $P < 0.01$) concerns Δt_c with *eo*.

Though the number of parameters in the Σ model is halved with respect to PWL model, the goodness of fit is slightly improved. In fact, the mean value of the RMSE computed over the thorough number of 240 trials changes from 0.15 for PWL to 0.09 for Σ. Also the change in the proportion of explained variance is confined within narrow limits.

3.3. Discriminant analysis

The following step in the development of the pattern recognition system dealt with the design of the classifier using the previously selected/extracted features and with the evaluation of the classifier performance using resubstitution and cross-validation (e.g., LOO) methods.

As regards the Σ model, maximal separability between groups was encountered in the plane *ec* vs *eo* of both parameters. Moreover, proportional relationships seem to exist between the *eo* and *ec* values of K and Δt_c such that for both groups, a Pearson correlation analysis discloses a significant collinearity between the *eo* and *ec* values of the parameters ($r > 0.76$, $P < 0.001$). This suggests that taking into account the Romberg ratios of K and Δt_c or, for similarity with CEA, their PDS, a further reduction in dimensionality can be pursued. Hence, classifier design was carried out on percentage difference of sway, PDS(.), in three cases (see Table 4), with either both or one single parameter.

As an example, Fig. 5 shows the LCOD in the plane $PDS(K) - PDS(\Delta t_c)$. In this case the misclassification probability computed with LOO (LOO%) was 6.7% (four subjects over 60), while the resubstitution error, that can be directly estimated from the figure, was 5% (three subjects over 60). Table 4 reports the performances of the classifiers, built upon different sets of parameters, and shows that the joint use of K and Δt_c has an added value with respect to their single contribution even if $PDS(K)$ (LOO% = 13.3) is more discriminant than $PDS(\Delta t_c)$ (LOO% = 30). This result can be read as further evidence that the two parameters of the Σ model are the prominent features of two different components of the SDF.

As regards the PWL model, classifier design was carried out on percentage difference of sway, PDS(.), in seven cases, with either all or all possible couples of parameters. Table 4 reports the misclassification error obtained

Table 4
Evaluation of the classifier for different sets of stochastic features

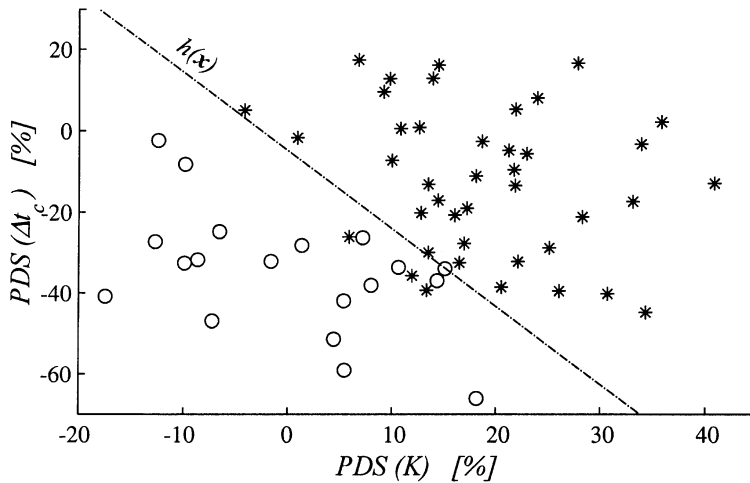| Model	Features	LOO%
Σ	$PDS(K)$, $PDS(\Delta t_c)$	6.7
	$PDS(K)$	13.3
	$PDS(\Delta t_c)$	30
PWL	$PDS(H_s)$, $PDS(K_s)$, $PDS(H_l)$, $PDS(K_l)$	16.6
	$PDS(H_l)$, $PDS(K_l)$	11.6

Fig. 5. The linear classifier in the plane of the Σ model parameters. Visual (∗) and Non-visual (○) subjects are shown. Three misclassified subjects can be directly seen (resubstitution error).

with all four PDS's (LOO% = 16.6) and the lowest error obtained within the six possible combinations of parameters two by two (LOO% = 11.6). It should be mentioned that this minimum was achieved with the long-term parameters H_l and K_l, while the worst performance (LOO% = 26.6) was accomplished by the pair of intercepts K_s and K_l. In this model the reduction of features gives rise to an advantage in term of misclassification error.

In summary, if we take the best results provided by either Σ or PWL model, the proposed method featuring the stochastic properties of the COP, gives very high performance in terms of pattern recognition capability. Nevertheless, if we compare the performances obtained in this task with the same number of features, the LOO% of Σ model is almost half the corresponding error ensured by PWL model. Hence, Σ model should be preferred for the classification of visual strategy.

If one looks separately at the single couples of consecutive *eo* and *ec* experiments, even in a repeated measurement setting, a certain amount of intra-subject variability can be noticed in the values of PDS(K) and PDS(Δt_c). Anyway, it seems not to affect the performance of the classifier. The consistency in time of the postural strategy together with the role of adaptation are now being investigated and will be object of a further study.

4. Discussion

Multivariate methods, such as statistical pattern recognition and discriminant analysis, in the past have proven to be useful instruments in managing and extracting information from the huge number of measurements acquired in movement analysis. These techniques have been utilized in the field of movement analysis to identify the most significant variables in different pathologies, and to design classification rules and quantitative evaluation scores. Gait patterns of patients with hip diseases (Yamamoto et al., 1983) and cerebral palsy (Kadaba et al., 1995) were assessed using principal component analysis. The extraction of functional scores allowed the pathological patterns to be discriminated from the normal ones. Stepwise discriminant analysis was used to classify normal and total knee replacement subjects and to develop knee and hip performance scores (Laughman, Stauffer, Ilstrup, & Chao, 1984; Chao, Kaufman, Cahalan, & Askew, 1988). Quantitative gait analysis and statistical pattern recognition were also used together as clinical decision-making aids in flat foot diagnosis and post-surgery monitoring (Bertani, Cappello, Benedetti, Simoncini, & Catani, 1999). Up to now few studies dealt with the pattern recognition of postural measurements. Nevertheless (i) the main contribution of vision on postural sway stabilization, and (ii) the relevant inter-individual differences in the results of the visual experiments were the object of several studies in the last decades.

(i) On one side, Kunkel, Freudenthaler, Steinhoff, Baudewig, and Paulus (1998) observed that, during visual stimulation with different spatial frequencies, sway velocity was reduced more efficiently by stabilizing visual frames than was root-mean-square (RMS) sway. Maki, Holliday, and Fernie (1987) explained the effect of visual deprivation on postural performances taking into account the stiffened control strategy, i.e. subjects might overcompensate for the loss of visual input by increasing the stiffness of the control system and hence the mean velocity of the sway. Since sway velocity is suggested to embody the dynamic muscle forces acting at the joints, it was argued that visual information can be used to reduce and therefore optimize dynamic muscle action even though static body sway is either not or less reduced.

We tested this hypothesis on the two groups of subjects that were identified according to the present classification scheme. Interestingly, we observed that PDS computed for RMS sway was significantly different ($P < 0.001$) between the non-visual (ω_1) and the visual (ω_2) groups. In particular, it was positive

for ω_2, meaning a greater RMS sway with *ec* than with *eo*, and negative for ω_1. This is not surprising since RMS sway and CEA are strongly correlated (Prieto et al., 1996). On the contrary, PDS computed for sway velocity was similar for ω_1 and ω_2 and always positive, to indicate a stabilizing effect of vision on dynamic muscle action, common to all subjects, irrespective of path traveled, that may depend on other factors, e.g. a different recruitment strategy among antigravitary muscles.

This is, to a certain extent, also in accordance with the results of Ishida and Imai (1980) that demonstrated increases in reflex gain when vision is deprived. In conclusion, one could think at the existence of a single response to the absence of visual input (i.e., similar mean velocities), in terms of stiffening, but this still does not mean that different choices can be made about the muscles to be stiffened or the timing (or spatial threshold) of the central controller (i.e., why RMS sway and CEA are different in the two groups?).

(ii) Several recent publications investigated the different patterns that could be encountered when visual expropriospecific information is challenged during posture. Casselbrant, Redfern, Furman, Fall, and Mandel (1998) studied the effect of a moving visual surrounding on the sway of children with otitis media and suggested that these subjects may be more visually dependent for balance than healthy age-matched controls. Jeka, Oie, and Kiemel (2000), testing healthy subjects under visual and somatosensory stimulation, observed three qualitatively distinct types of sensory integration, one of which was defined vision dominant for the prevalence of visual information with respect to other sensory modalities. Isableu, Ohlmann, Cremieux, and Amblard (1997), analyzing the different postural performances of subjects improving their balance with the aid of visual cues and other not doing so, assumed that the responsible for this discrepancy were the processes involved in selecting and/or controlling the spatial frame of reference. The well-known inter-individual differences described in the perception of verticality, and particularly in the perceived orientation of the body in space, could explain the postural variability.

Spontaneous sway studies have also shown that eye closure results in increased sway in most but not all healthy subjects. Different proportions of these visual healthy subjects were identified up to now in literature, ranging from 54% (Lacour et al., 1997) to 90% (Black et al., 1982). Indeed, several additional factors can affect this variability including the recording conditions (e.g., the different role that adaptation can play over different experimental designs), the experimental setup (e.g., the distance from the visual target and its shape), the scores employed to quantify sway. This latter aspect

should be carefully considered since different scores could describe different aspects of the postural performance.

Collins and De Luca (1995) identified two visual strategies, sharing the muscular stiffness decrease as the main effect of visual integration, on the basis of the characteristics of SDF's. They substantially differentiated subjects according to the RQ of the planar long-term effective diffusion coefficient and the resulting groups can be associated to our groups since the qualitative properties of the respective SDF are very similar. Hence, they argued that, for visual subjects, visual input reduces the stiffness by decreasing the level of muscular activity across the joints. On the contrary, non-visual subjects' sway seems to reflect a reweighing of the sensory loops (visual, vestibular, proprioceptive) in postural control.

The discriminant analysis carried out in the present paper on the PWL parameters confirms the observation made by Collins and De Luca (even if they did not support it by an analytical pattern recognition approach) that the long-term stochastic parameters play a major role in discriminating the visual and non-visual subjects (see Table 4). Similar conclusions concern H_l, decreasing significantly in both groups when eyes are closed, but not H_s that here is significantly increased by visual input in group ω_1.

As concerns the new model, the two parameters seem to suggest that the opposite trend in the size of body sway observed upon eye closure, could be explained by a different modulation of their interplay. In fact, both K and Δt_c have changes of the same sign when eyes get closed, but such changes have different levels of significance. In particular, the visual feedback contributes to a general reduction in K, a diffusion coefficient that may be thought in part as a measure of muscle stiffness. In this respect, the correlation found between K and mean velocity (Spearman rank correlation coefficient $r = 0.86$), is noteworthy.

The increase in Δt_c observed in the eo condition is instead symptom of a later transition between persistent and antipersistent behavior due to the visual feedback. This may reflect (see Fig. 2) an increase in the difference in variance (power) between the bands below and above 1 Hz, with an increase over the low frequencies. This result is consistent with the spectral contribution of the visual afference to postural control, which was located at about 0.2 Hz (Yoshizawa, Takeda, Ozawa, & Sasaki, 1992).

Stabilogram diffusion plots, representative of the two populations, are shown in Fig. 6. Once more, they emphasize the fact that ω_1 and ω_2 have pretty similar SDF with *ec*, and the greatest part of the between-group difference can be inferred by looking at the SDF with *eo*. In this condition the
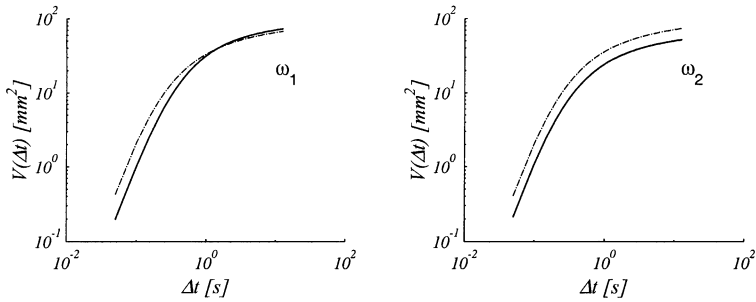
Fig. 6. Representative SDF for the Non-visual (ω_1) and Visual (ω_2) subjects. The comparison is proposed between the eo (solid line) and ec conditions (dotted line).

SDF of ω_1 are stretched upward (K is commonly higher than in ω_2) and less flat for high lags (due to the larger values of Δt_c). This result shows that in the non-visual group (ω_1) the difference between *eo* and *ec* is really marginal, so that at a first glance the outcome of the postural control system seems completely insensitive to the visual feedback. As a matter of fact the muscle stiffness with *eo* is very high in this case, but the transition time very delayed. For this reason it would be probably inefficient to control posture by further increasing stiffness upon eye closure, and the role of maintaining oscillations in an acceptable range could be demanded to an advance in the transition between persistence and antipersistence. Many factors could contribute to this aim, including changes in physical parameters such as inertial movement and bounding (Liebovitch & Yang, 1997). This action determines a significant reduction in the stochastic activity for high lags, and hence a more accurate control when eyes are closed than when eyes are open. On the contrary, the visual group (ω_2) shows the expected increase in muscle stiffness upon eye closure, which contributes the greatest part of the control. Only a residual role is played here by a less prominent advance in the transition.

It should be remarked that the values of Δt_c which are estimated with the new technique are significantly lower than the values of τ in the PWL model (they can be computed with Eq. (11) and are around 0.9 seconds) and the values reported by Collins and De Luca (1995). Nevertheless, they are consistent with experimental observations in motor control feedback studies, and are comparable with the transition times recently estimated by Rougier (1999) with an automatic technique aimed at determining the two successive portions of the SDF.

But which is the link between the new parameters, K and Δt_c, and the parameters of the PWL model? It can be verified, by expanding Eq. (8)

around $\Delta t_c \pm \varepsilon$, with ε small but finite, that the ratios H_s/H_l and K_s/K_l are uniquely identified once Δt_c is given. In other words, Δt_c summarizes all the information concerning the "change in scaling" from short to long latencies.

As regards K, it is obviously related to the values of K_s and K_l of the PWL model (Spearman rank correlation coefficients: $r = 0.88$ and $r = 0.78$, respectively; $P < 0.0001$).

PDS(K) and PDS(Δt_c) are significantly different in the two populations ($P < 0.001$) and on the average their absolute values are greater in ω_2 than in ω_1 for K, and greater in ω_1 (more negative) than in ω_2 for Δt_c. The high values of Δt_c estimated in ω_1 when eyes are open, suggest a greater variance on the large time-lags and hence the presence of a more significant low-frequency component in the sway. This could reflect a different kind of exploration of the base of support requiring longer times to be stabilized.

A final remark concerns the comparison with other models proposed in the literature, and in particular with the model used by Newell et al. (1997), which has the same number of parameters as the new one. The two parameters of the linear Ornstein–Uhlenbeck (OU) process, namely a diffusion and a drift coefficient, were estimated and matched with the best set of features provided by the new model ($K, \Delta t_c$). To compare these different models, a measure of their "goodness" is required. A logical approach is to evaluate both their ability to fit the experimental SDF, and the expected accuracy of the parameter estimates. Moreover, the performance of the classifiers built upon the two sets of features can be checked. The former aspects were assessed by the: (i) RMSE – the new method better fits the SDF (0.09 vs 0.12), and (ii) mean radius of the circle equivalent to the indifference ellipse in the parameter space – this radius represents the mean relative error and is expressed as a percentage; the parameters of the new method are more accurate (7.1% vs 8.4%). Finally, classifiers based on the PDS of the two sets of features were evaluated by the LOO error. Once again model Σ performed better than the OU model (LOO 6.6% vs 8.3%). Hence, the new method parallels (or slightly improves) the results provided by the OU with the same number of features.

5. Conclusions

Many studies in patients with a variety of disorders affecting the afferent pathways (i.e., visual, vestibular, somatosensory) suggest that posturography might be a useful clinical tool for evaluating balance problems. But whether

static posturography is sensitive enough to enlighten on the performances and the different strategies of the postural control system in normal conditions is still an open question. For this reason a new method that seems appropriate to describe the fractal properties of the COP was developed and tested. The new model of the stochastic process is based on the assumption that different scaling laws can be identified on the basis of time-scale dependent parameters.

The purpose of this study was to evaluate the sensitivity of such a model to the visual strategies put into play in a population of healthy subjects and to compare its performances with stochastic models previously proposed in literature. New parameters were compared with the previous ones, in terms of visual strategy pattern recognition and sensitivity to operating conditions during the classic Romberg test. The overall framework that was designed seemed robust and reliable for classification mainly due to the new feature extraction scheme based on data modeling of the COP time-series.

Obtained results seem encouraging of the possibility of achieving discriminant information about postural ability from the COP time-series itself. Nevertheless, further insight on the physiological meaning of the new parameters will help in improving both their experimental impact and analytical aspects.

References

Bassingthwaighte, J. B., Liebovitch, L. S., & West, B. J. (1994). *Fractal physiology*. Oxford: Oxford University Press.

Benassi, A., & Deguy, S. (1999). *Multi-scale fractional Brownian motion: Definition and identification*. Technical Report 83, LLAIC1, Laboratoire de Logique, Algorithmique et Informatique de Clermont 1, France.

Bertani, A., Cappello, A., Benedetti, M. G., Simoncini, L., & Catani, F. (1999). Flat foot functional evaluation using pattern recognition of ground reaction data. *Clinical Biomechanics*, *14*, 484–493.

Bezdek, J. C. (1981). *Pattern recognition with fuzzy objective function algorithms*. New York: Plenum Press.

Bezdek, J. C. (1998). Pattern analysis. In W. Pedrycz, H. E. Ruspini, & P. P. Bonissone (Eds.), *Handbook of fuzzy computation* (pp. F6.1:1–F6.6:20). Philadelphia: Institute of Physics Publishing.

Black, F. O. (1982). Vestibular function assessment in patients with Meniere's disease: The vestibulospinal system. *Laryngoscope*, *92*, 1419–1436.

Black, F. O., Wall, C., Rockette, H. E., & Kitch, R. (1982). Normal subject postural sway during the Romberg test. *American Journal of Otolaryngology*, *3*, 309–318.

Casselbrant, M. L., Redfern, M. S., Furman, J. M., Fall, P. A., & Mandel, E. M. (1998). Visual-induced postural sway in children with and without otitis media. *Annals of Otology, Rhinology and Laryngology*, *107*, 401–405.

Chao, E. Y., Kaufman, K. R., Cahalan, T. D., & Askew, L. J. (1988). Comparison of objective gait analysis and clinical evaluation after total hip arthoplasty. In R. H. Fitzgerald, *Non-cemented total hip arthoplasty* (pp. 323–334). New York: Raven Press.

Chiari, L., Cappello, A., Lenzi, D., & Della Croce, U. (2000). An improved technique for the extraction of stochastic parameters from stabilograms. *Gait and Posture*, *12* (3), 225–234.

Chow, C. C., Lauk, M., & Collins, J. J. (1999). The dynamics of quasi-static posture control. *Human Movement Science*, *18*, 725–740.

Collins, J. J., & De Luca, C. J. (1993). Open-loop and closed-loop control of posture: A random-walk analysis of center-of-pressure trajectories. *Experimental Brain Research*, *95*, 308–318.

Collins, J. J., & De Luca, C. J. (1995). The effects of visual input on open-loop and closed-loop postural control mechanisms. *Experimental Brain Research*, *103*, 151–163.

Dichgans, J., Mauritz, K. H., Allum, J., & Brandt, T. (1976). Postural sway in normals and atactic patients: Analysis of the stabilizing and destabilizing effects of vision. *Agressologie*, *17*, 15–24.

Duarte, M., & Zatsiorsky, V. M. (2000). On the fractal properties of natural human standing. *Neuroscience Letters*, *283*, 173–176.

Fitzpatrick, R., & McCloskey, D. I. (1994). Proprioceptive, visual and vestibular thresholds for the perception of sway during standing in humans. *Journal of Physiology (London)*, *478* (Pt 1), 173–186.

Fukunaga, K. (1990). *Introduction to statistical pattern recognition*. London: Academic Press.

Gagey, P. M., & Toupet, M. (1991). Orthostatic postural control in vestibular neuritis: A stabilometric analysis. *Annals of Otology, Rhinology and Laryngology*, *100*, 971–975.

Horak, F. B., Shupert, C. L., Dietz, V., & Horstmann, G. (1994). Vestibular and somatosensory contributions to responses to head and body displacements in stance. *Experimental Brain Research*, *100*, 93–106.

Hurst, H. E. (1951). Long-term storage capacity of reservoirs. *Transactions of the American Society of Civil Engineers*, *116*, 770–808.

Inglis, J. T., Horak, F. B., Shupert, C. L., & Jones-Rycewicz, C. (1994). The importance of somatosensory information in triggering and scaling automatic postural responses in humans. *Experimental Brain Research*, *101*, 159–164.

Isableu, B., Ohlmann, T., Cremieux, J., & Amblard, B. (1997). Selection of spatial frame of reference and postural control variability. *Experimental Brain Research*, *114*, 584–589.

Ishida, A., & Imai, S. (1980). Responses of the posture-control system to pseudorandom acceleration disturbances. *Medical and Biological Engineering and Computing*, *18*, 433–438.

Jeka, J. J., Oie, K., & Kiemel, T. (2000). Multisensory information for human postural control: Integrating touch and vision. *Experimental Brain Research*, *134*, 107–125.

Kadaba, M. P., Ramakrishnan, H. K., Jacobs, D., Chambers, C., Scarborogh, N., & Goode, B. (1995). Pattern recognition in spastic diplegia. *Biomecánica*, III, 49–58.

Kaufman, L., & Rousseeuw, P. J. (1990). *Finding groups in data: An introduction to cluster analysis*. New York: Wiley.

Kunkel, M., Freudenthaler, N., Steinhoff, B. J., Baudewig, J., & Paulus, W. (1998). Spatial-frequency-related efficacy of visual stabilisation of posture. *Experimental Brain Research*, *121*, 471–477.

Lacour, M., Barthelemy, J., Borel, L., Magnan, J., Xerri, C., Chays, A., & Ouaknine, M. (1997). Sensory strategies in human postural control before and after unilateral vestibular neurotomy. *Experimental Brain Research*, *115*, 300–310.

Laughman, R. K., Stauffer, R. N., Ilstrup, D. M., & Chao, E. Y. (1984). Functional evaluation of total knee replacement. *Journal of Orthopaedic Research*, *2*, 307–313.

Liebovitch, L. S., & Yang, W. (1997). Transition from persistent to antipersistent correlation in biological systems. *Physical Review E*, *56* (4), 4557–4566.

Maki, B. E., Holliday, P. J., & Fernie, G. R. (1987). A posture control model and balance test for the prediction of relative postural stability. *IEEE Transactions on Biomedical Engineering*, *34*, 797–810.

Mandelbrot, B. B., & Van Ness, J. W. (1968). Fractional Brownian motions, fractional noises and applications. *SIAM Review*, *10*, 422–437.

Marucchi, C., & Gagey, P. M. (1987). Postural blindness. *Agressologie*, *28*, 947–948.

Mittelstaedt, H. (1996). Somatic graviception. *Biological Psychology*, *42*, 53–74.

Myklebust, J. B., Prieto, T., & Myklebust, B. (1995). Evaluation of nonlinear dynamics in postural steadiness time series. *Annals of Biomedical Engineering*, *23*, 711–719.

Newell, K. M., Slobounov, S. M., Slobounova, E. S., & Molenaar, P. C. (1997). Stochastic processes in postural center-of-pressure profiles. *Experimental Brain Research*, *113*, 158–164.

Prieto, T. E., Myklebust, J. B., Hoffmann, R. G., Lovett, E. G., & Myklebust, B. M. (1996). Measures of postural steadiness: Differences between healthy young and elderly adults. *IEEE Transactions on Biomedical Engineering*, *43*, 956–966.

Riley, M. A., Wong, S., Mitra, S., & Turvey, M. T. (1997). Common effects of touch and vision on postural parameters. *Experimental Brain Research*, *117*, 165–170.

Rougier, P. (1999). Influence of visual feedback on successive control mechanisms in upright quiet stance in humans assessed by fractional Brownian motion modeling. *Neuroscience Letters*, *266*, 157–160.

Van Parys, J. A., & Njiokiktjien, C. J. (1976). Romberg's sign expressed in a quotient. *Agressologie, 17 SPECNO*, 95–99.

Xie, X. L., & Beni, G. (1991). A validity measure for fuzzy clustering. *IEEE Transactions on Pattern Analysis and Machine Intelligence*, *13*, 841–847.

Yamamoto, S., Suto, Y., Kawamura, H., Hashizume, T., Kakurai, S., & Sugahara, S. (1983). Quantitative gait evaluation of hip diseases using principal component analysis. *Journal of Biomechanics*, *16*, 717–726.

Yoshizawa, M., Takeda, H., Ozawa, M., & Sasaki, Y. (1992). A frequency domain hypothesis for human postural control characteristics (visual feedback). *IEEE Engineering in Medicine and Biology Magazine*, *11*, 59–63.